Received 30 August 2023; revised 20 October 2023; accepted 8 November 2023. Date of publication 15 November 2023;
date of current version 6 December 2023. The review of this article was arranged by Editor A. Nathan.

Digital Object Identifier 10.1109/JEDS.2023.3332894

A Low-Temperature Poly-Silicon Thin Film Transistor Pixel Circuit for Active-Matrix Simultaneous Neurostimulation

TAOMING GUO [1] (Graduate Student Member, IEEE), BOWEN LIU [1], JIWEI ZOU [1], HANBIN MA [2,3] (Member, IEEE), YONGPAN LIU [1] (Senior Member, IEEE), XUEQING LI [1] (Senior Member, IEEE), HUAZHONG YANG [1] (Fellow, IEEE), AND CHEN JIANG [1] (Member, IEEE)

1 Department of Electronic Engineering, Tsinghua University, Beijing 100084, China
2 CAS Key Laboratory of Bio Medical Diagnostics, Suzhou Institute of Biomedical Engineering and Technology, Suzhou 215163, China
3 Guangdong ACXEL Micro Nano Tech Company Ltd., Foshan 528200, China

CORRESPONDING AUTHOR: C. JIANG (e-mail: chenjiang@tsinghua.edu.cn)

This work was supported in part by the National Natural Science Foundation of China under Grant 82151305 and Grant 62374102, and in part by Lingang Laboratory under Grant LG-QS-202202-09.

ABSTRACT This work reports a novel low-temperature poly-silicon thin-film-transistor-based pixel circuit for active-matrix neurostimulation. The pixel circuit consists of four transistors and one capacitor (4T1C) for programmable current-mode stimulation, which are designed for storing stimulation intensity information, simultaneously stimulating a large number of channels, and discharging stimulation electrodes. Due to the high mobility and low threshold voltages of the devices, the fabricated circuit occupies a pixel area of 200 × 200 μm^2, and delivers a stimulation current of 147 μA, sufficient to stimulate a neuron. The turn-on resistance of the fabricated transistor is below 6 $k\Omega$, sufficient to be used as switches for bioelectronic applications. By employing a discharging switch transistor, the accumulated charges on the stimulation electrodes were released, and the electrode voltage was reduced to 0.08 V, thus mitigating corrosion. We demonstrated that two pixel circuits at different rows and columns can output stimuli simultaneously without a noticeable delay. This pixel circuit shows high potential to scale up as an active-matrix neurostimulation system with a high channel count.

INDEX TERMS Active matrix, neurostimulation, simultaneous stimulation, thin film transistors.

I. INTRODUCTION

Recent advances in brain-computer interfaces show a promising prospect for integrating biological tissue with electronic devices, especially in neurostimulation [1], [2], [3]. To interface neural tissue directly, thin film transistors (TFTs) are potential for flexible and large-area bioelectronic systems [4], [5], compared to highly integrated CMOS chips. By using TFT matrix as switches (i.e., a 1T0C pixel circuit), high-channel-count neurostimulation systems can be achieved [6], which is a bottleneck in conventional neurostimulators that use the one-to-one wiring scheme [7], [8], [9]. However, in the state of the art of TFT-based neurostimulation, the 1T0C pixel circuit only stimulate neurons when addressed. In other words, this TFT switch matrix is passive and cannot support simultaneous stimulation at different rows or columns. Therefore, it is appealing to introduce an active-matrix method for neurostimulation, similar to the way high-resolution active-matrix displays are achieved [10], [11].

For neurostimulation, there are some specific requirements for devices and circuits. Typical stimulation signals are rectangular current pulses [12], [13], and neurons respond differently according to the magnitude of the pulses (1 - 100 μA) [14]. Besides, a simultaneous stimulation matrix

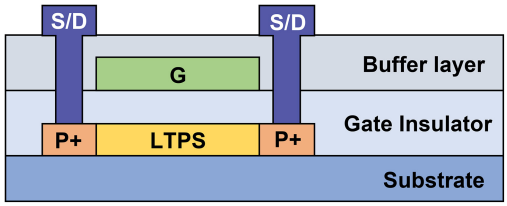

FIGURE 1. Cross-sectional view of the fabricated p-type LTPS TFTs. S/D stands for source and drain, and G stands for gate.

ensures that the neurostimulator can deliver different patterns and stimulate neurons at different positions without delay. In addition, stimulation pulses can cause charge accumulation between electrodes and eventually result in reduction and/or oxidation on the electrodes [15]. To solve this problem, a method for stimulation with discharge is required [16]. Taking these into account, for a neurostimulation matrix, programmability, discharge, and simultaneity are essential requirements for proper stimulation. These further require TFTs to have high mobility, low threshold voltage, and high on/off ratio, to sufficiently stimulate neurons at low operating voltages and reduce background stimulation noise [17], [18].

In this work, we demonstrate a novel 4T1C pixel circuit for active-matrix simultaneous neurostimulation, using a low-temperature poly-silicon (LTPS) TFT technology. The operation of the circuit takes the advantages of the fabricated LTPS TFTs and has been verified with measured results. This LTPS TFT pixel circuit for the first time enables a neurostimulation matrix to program pixel stimulation intensity independently, output stimuli simultaneously, and discharge stimulation electrodes, which are the key requirements for high-channel-count neurostimulation.

II. LTPS FABRICATION AND PROPOSED PIXEL CIRCUIT

A. FABRICATION OF LTPS TFTS

The fabricated p-type LTPS TFTs use a top-gate self-aligned structure, as shown in Fig. 1. This structure could significantly reduce parasitic capacitance, important for TFT circuit implementation for neurostimulation applications. For device fabrication, a layer of poly-silicon was deposited on the glass substrate, followed by the channel area with an n-doping process. A SiO_x layer was deposited by plasma-enhanced chemical vapor deposition without patterning, as the gate insulator. The gate metal Mo was deposited and patterned by photolithography. Using the gate metal as the hard mask, the poly-silicon was highly p-doped to form the source and drain electrodes, rendering a self-aligned structure. After deposition of a SiO_x buffer layer, vias were etched for connection of source and drain metal. Finally, a trilayer of Ti/Al/Ti was deposited as source and drain contacts. The devices were characterized by a Keysight B1500A Semiconductor Device Parameter Analyzer.

B. OPERATION OF PROPOSED CIRCUIT

The proposed circuit comprises four transistors and one capacitor as shown in Fig. 2(a). T_{sel} is the switch addressed

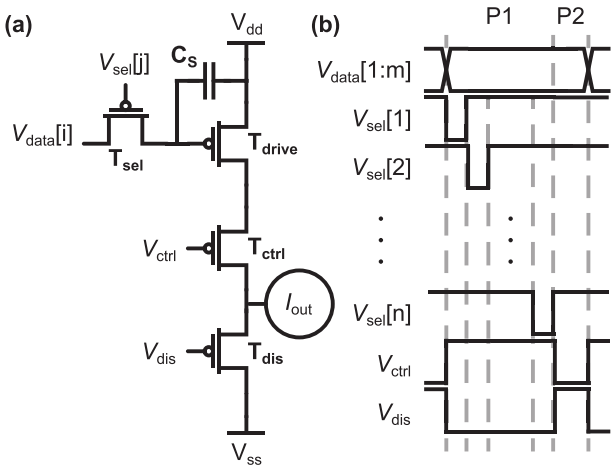

FIGURE 2. (a) Schematic and (b) timing diagram of the proposed 4T1C stimulation pixel circuit. P1 and P2 stand for phase (1) and phase (2) in a stimulation cycle.

by selection lines ($V_{sel}[j]$) to program voltages on data lines ($V_{data}[i]$) to the storage capacitor C_s. T_{drive} is the driving transistor to provide the stimulation electrodes with current. T_{ctrl} is the switch to control the output of the stimulation pixel. T_{dis} is the switch to ground the stimulation electrode and release the accumulated charges.

Fig. 2(b) illustrates the timing diagram of the proposed circuit. Each stimulation cycle includes two phases. During phase (1), the programming and discharging processes are carried out concurrently. T_{sel} is turned on when $V_{sel}[j]$ is low, and the stimulation intensity on $V_{data}[i]$ is written in C_s. Unlike the line-by-line programming of the data/selection lines, all T_{dis} of the matrix is turned on for all the stimulation electrodes to discharge for the longest possible period. By turning off T_{ctrl}, the programming and discharging operations are isolated to prevent interference between them.

In phase (2), T_{sel} and T_{dis} are turned off, and T_{ctrl} is turned on. T_{drive} operates in the saturation region as a current source, and all T_{ctrl} of the matrix are turned on at the same time to ensure that all pixels provide current stimuli simultaneously. The stimulation intensity (i.e., the current of T_{drive}) is modulated by the voltage data stored in the C_s.

III. EXPERIMENTAL RESULTS AND DISCUSSIONS

A. DEVICE CHARACTERIZATION

The electrical characteristics of a typical transistor with a channel *W/L* (width-to-length ratio) of 20 μm / 4 μm are shown in Fig. 3(a,b). The p-type TFT presented an on/off ratio of 10^7 and a threshold voltage of –0.52 V at the drain voltage (V_{DS}) of –10 V. The large on/off ratio is important to achieve active-matrix neurostimulation without background stimulation noise. The mobility of the p-type transistor was 72.9 $cm^2/V \cdot s$, which guarantees sufficient current for neurostimulation. As shown in Fig. 3(b), the output characteristics of the TFT show a high current (>100 μA, sufficient for electrical neurostimulation [19]) in saturation region at low voltages ($|V_{GS}| < 6$ V, $|V_{DS}| < 5$ V) and a large

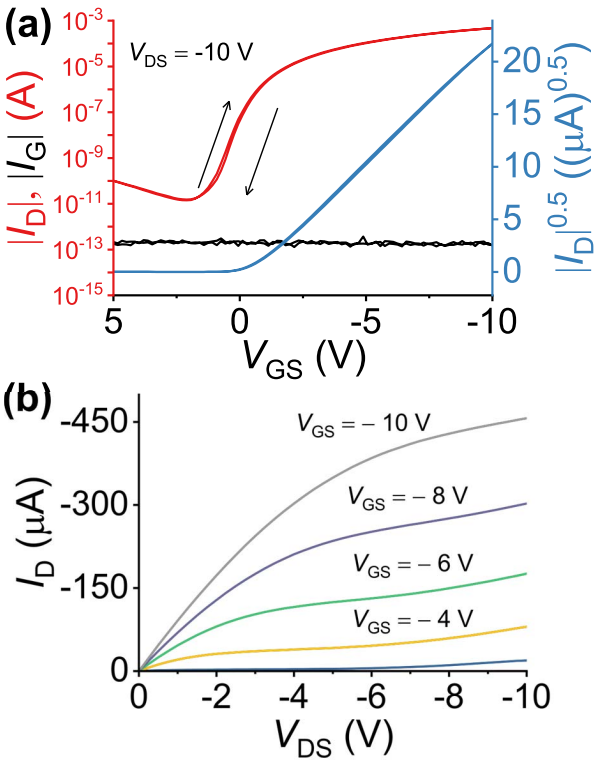

FIGURE 3. (a) Transfer and (b) output characteristics of a typical LTPS TFT (W/L = 20 μm / 4 μm).

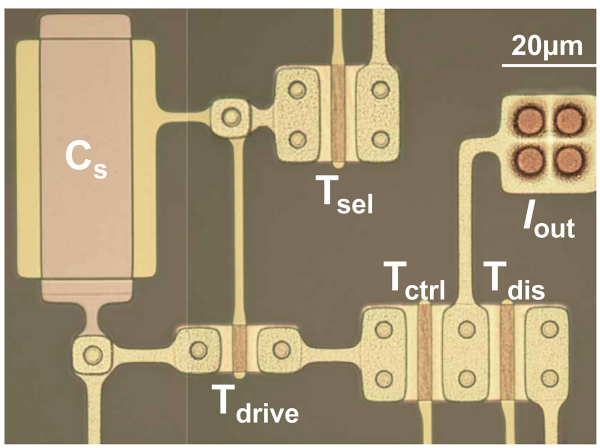

FIGURE 4. Microscopic photo of the fabricated 4T1C pixel circuit.

Early voltage of 20.6 V. The pixel circuit was fabricated with a p-type LTPS TFT technology, and the circuit operation was verified with measured results. The sizes of T_{sel}, T_{ctrl}, T_{dis} were 20 μm / 4 μm, T_{drive} was 10 μm /4 μm and C_s was 1000 μm^2, as shown in Fig. 4. The pixel circuit occupies a small area of 200 × 200 μm^2, which is comparable with the pixel area of typical neural electrodes (e.g., Utah Array). Such small area can be attributed to the high mobility of LTPS TFTs.

B. STIMULATION PROPERTIES OF THE PIXEL CIRCUIT

We characterized the function of the fabricated circuit as a neural stimulator pixel, as shown in Fig. 5. The gate

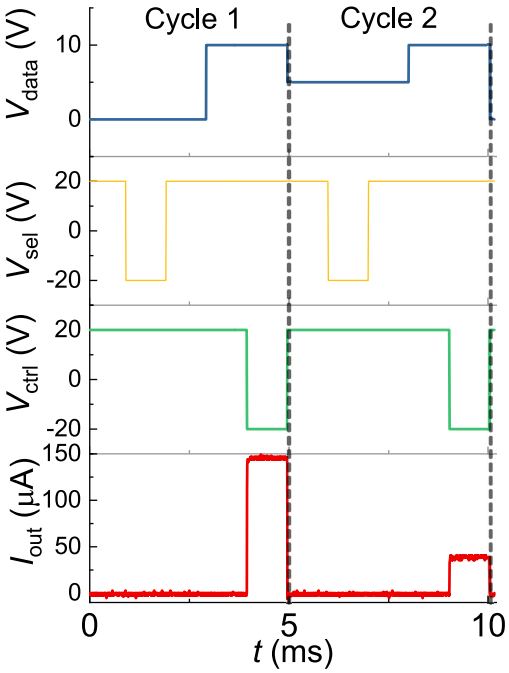

FIGURE 5. Measured output current (I_{out}) of fabricated pixel circuit as function of time.

voltages of T_{sel} and T_{ctrl} transistor switches were toggled between 20 V and –20V, to bias the transistors in the cut-off region and linear region, respectively. The linear region operation for the on-state was to ensure low resistances for the transistor switches, and thus the output current (I_{out}) is mainly determined by the gate voltage of T_{drive} (i.e., the stored voltage data). Two different data voltages of 0 V and 5 V were programmed through the data line. As shown in Fig. 5, the control signal (V_{ctrl}) effectively controls the on- and off-states of I_{out}, while the level of I_{out} can be modulated by data signal (V_{data}) on the gate of T_{drive}. Specifically, two different stimulation current intensities of 147 μA and 35 μA were observed (Fig. 5).

The I_{out}–V_{data} relation was further characterized by sweeping V_{data}, while keeping T_{sel}/T_{ctrl} on and T_{dis} off. As shown in Fig. 6(a), a quadratic relation was observed, which can be attributed to the operation of T_{drive} in the saturation region. This saturation region operation also guarantees that the pixel circuit acts as a current source, stabilizing the output current regardless of the changes in load impedance. This is particularly important for biomedical applications, since the impedance changes variably at the electrode/electrolyte interfaces [20], due to the unstable biochemical environments. Fig. 6(b) illustrates that the output current remained 41 μA when output resistance R_{out} = 100 kΩ (maximum output current 48 μA). This flat output characteristics can tolerate biological impedance changes between 1kΩ and 100 kΩ without significant output current change (< 20%), as compared to a voltage source scheme with a large fluctuation of 99%. Indeed, the tolerance was enabled by the saturation characteristics of the fabricated LTPS TFT, which could be

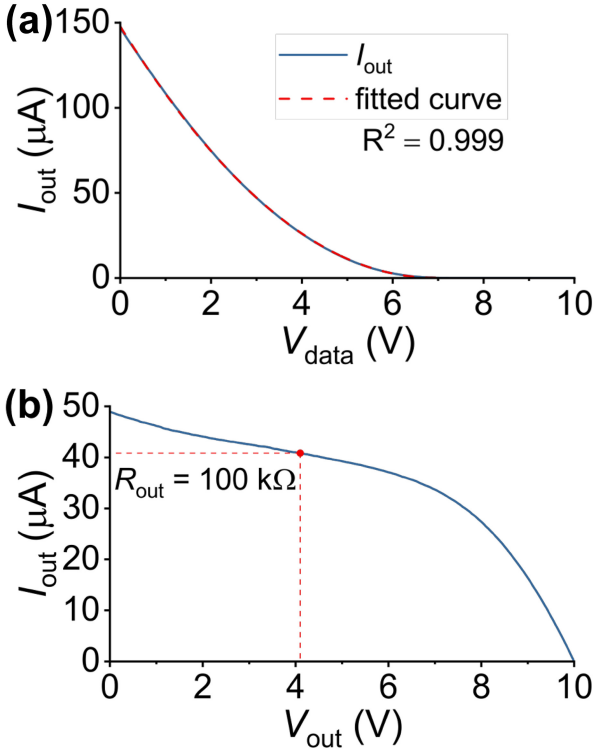

FIGURE 6. (a) Measured I_{out} under different voltage data (V_{data}). (b) Output characteristics of the pixel circuit at V_{data} = 3 V.

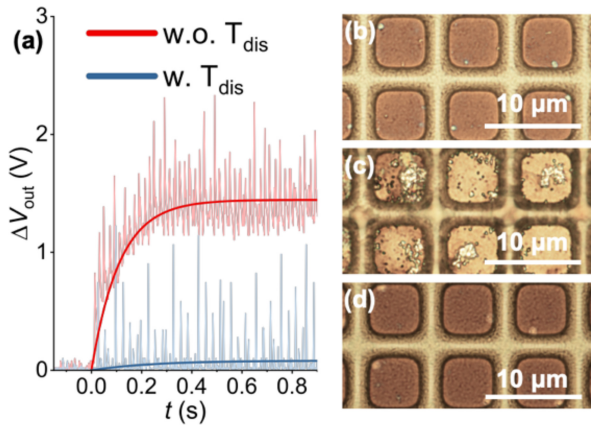

FIGURE 7. (a) Measured voltages of the stimulation electrodes with and without a discharging transistor (T_{dis}), under pulsed stimulation. The bold lines show the smoothed voltage over time. (b-d) Microscopic photos of the electrodes (b) before stimulation, (c) after stimulation without T_{dis} discharging, and (d) after stimulation with T_{dis} discharging. The squares are indium-tin-oxide electrodes.

further improved by a larger channel length or a thinner semiconductor layer.

C. DISCHARGING FUNCTION OF THE PIXEL CIRCUIT

The damage to stimulation electrodes was mitigated by adding a discharging transistor. Fig. 7(a) shows the measured voltage of stimulation electrodes with and without a discharging transistor, T_{dis}. The stimulation (V_{data} = 5 V) lasted 1 ms, followed by a relaxation of 4 ms. The short relaxation

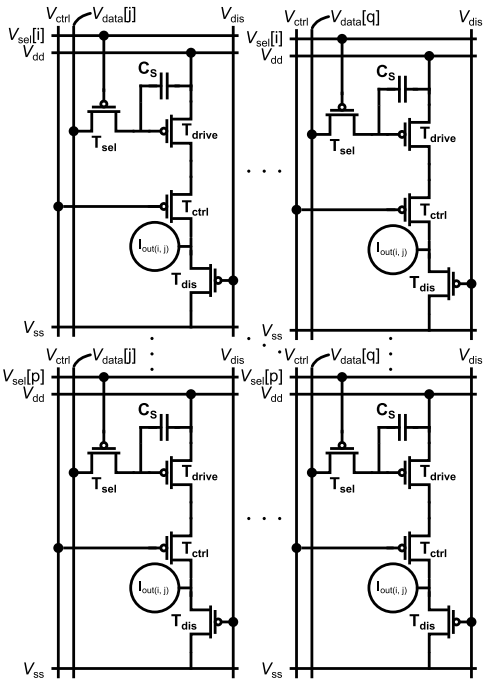

FIGURE 8. Schematic of a 4T1C active-matrix stimulation array.

was intended to expedite the corrosion of the stimulation electrodes. The electrodes were soaked in the normal saline to simulate a biological environment. For both cases with and without T_{dis}, we observed spikes in the measured voltages of the stimulation electrodes, as shown in Fig. 7(a). These spikes resulted from the charging and discharging of the electrodes under stimulation and relaxation, due to the resistive and capacitive nature of the electrode/electrolyte interfaces. The voltages of the electrodes were smoothed over time to show the trend of voltage shift. Without T_{dis}, the smoothed voltage increased at the starting cycles and saturated at 1.45 V. Such a high DC bias can accelerate the corrosion of the electrodes. In comparison, with T_{dis} releasing the accumulated charges, the averaged voltage was 0.08 V, which lowered the probability of electrode corrosion. The mitigated damage was confirmed by the optical microscopic photos of the electrodes before and after 5-min stimulation (Fig. 7(b)-(d)). The electrodes without T_{dis} discharging showed obvious physical damage with holes, while the electrodes with T_{dis} discharging remained visibly intact. Such fast discharging was enabled by the low on-state resistance of the fabricated LTPS TFT (∼ 5 kΩ). Therefore, it is important that the devices possess a high mobility to act as a good switch for bioelectrode discharging.

D. IMPLEMENTATION OF AN ACTIVE-MATRIX STIMULATOR

The pixel circuit was implemented to a matrix as shown in Fig. 8. The control signal and discharging signal were connected to every pixel, to achieve the simultaneous operation of output and discharge for all pixels. The simultaneous

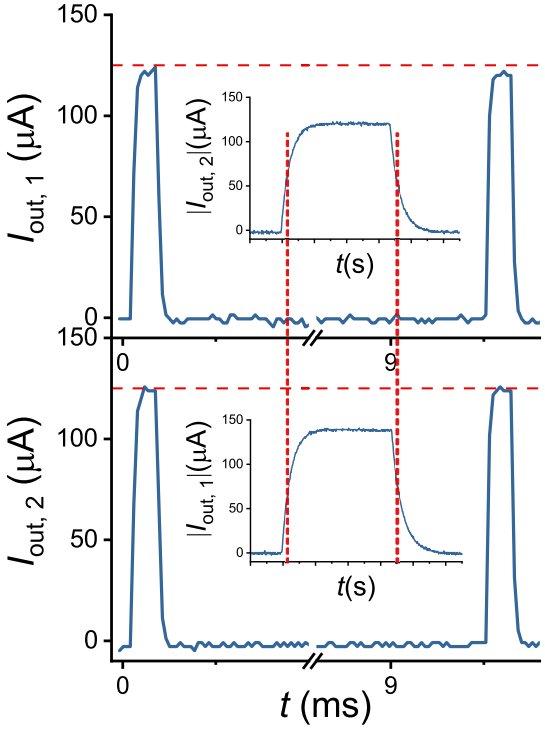

FIGURE 9. Measured output current of two independent pixel circuits as a function of time. Inset: output current in a zoomed-in time scale.

stimulation of two different pixel circuits from different rows and columns was demonstrated. After programming all pixel circuits, the stimulation current output simultaneously as designed as shown in Fig. 9. The circuit showed a rise time of 8 μs and a fall time of 13 μs, without a noticeable delay between the two pixels. The rise/fall times are relatively short compared to typical stimulus, of which the pulse duration is normally about 50-100 μs. The short rise/fall times and unnoticeable delay can be attributed to the self-aligned structure of the fabricated LTPS TFTs.

IV. CONCLUSION

This work presents a pixel circuit for active-matrix neurostimulation using LTPS TFTs. Compared to the conventional one-to-one wiring scheme, the 4T1C design can upscale channel counts by orders of magnitude. By implementing the circuit with LTPS TFTs, this work for the first time demonstrated a current stimulation pixel circuit which allows a neurostimulation matrix outputs stimuli simultaneously at different rows and columns, and programs the stimulation intensity independently. We expect that the proposed TFT active matrix would provide a promising solution for large-area and high-channel-count neurostimulation.

ACKNOWLEDGMENT

The authors gratefully acknowledge the assistance of TIANMA Microelectronics Corp. for manufacturing the chips in the Multi Project Glass platform.

REFERENCES

[1] E. Lowet et al., "Deep brain stimulation creates informational lesion through membrane depolarization in mouse hippocampus," *Nat. Commun.*, vol. 13, no. 1, Dec. 2022, Art. no. 7709, doi: 10.1038/s41467-022-35314-1.
[2] J. Lee et al., "Neural recording and stimulation using wireless networks of microimplants," *Nat. Electron*, vol. 4, no. 8, pp. 604–614, Aug. 2021, doi: 10.1038/s41928-021-00631-8.
[3] F. B. Wagner et al., "Targeted neurotechnology restores walking in humans with spinal cord injury," *Nature*, vol. 563, no. 7729, pp. 65–71, Nov. 2018, doi: 10.1038/s41586-018-0649-2.
[4] S. Wang et al., "Skin electronics from scalable fabrication of an intrinsically stretchable transistor array," *Nature*, vol. 555, no. 7694, pp. 83–88, Mar. 2018, doi: 10.1038/nature25494.
[5] H. Oh, J.-Y. Oh, C. W. Park, J.-E. Pi, J.-H. Yang, and C.-S. Hwang, "High density integration of stretchable inorganic thin film transistors with excellent performance and reliability," *Nat. Commun.*, vol. 13, no. 1, Aug. 2022, Art. no. 4963. doi: 10.1038/s41467-022-32672-8.
[6] F. A. Shaik, S. Ihida, Y. Ikeuchi, A. Tixier-Mita, and H. Toshiyoshi, "TFT sensor array for real-time cellular characterization, stimulation, impedance measurement and optical imaging of in-vitro neural cells," *Biosens. Bioelectron.*, vol. 169, Dec. 2020, Art. no. 112546. doi: 10.1016/j.bios.2020.112546.
[7] D.-H. Kim et al., "Dissolvable films of silk fibroin for ultrathin conformal bio-integrated electronics," *Nat. Mater.*, vol. 9, no. 6, pp. 511–517, Jun. 2010, doi: 10.1038/nmat2745.
[8] B. J. Woodington et al., "Electronics with shape actuation for minimally invasive spinal cord stimulation," *Sci. Adv.*, vol. 7, no. 26, Jun. 2021, doi: 10.1126/sciadv.abg7833.
[9] D. C. Rodger et al., "High-density flexible parylene-based multi-electrode arrays for retinal and spinal cord stimulation," in *Proc. TRANSDUCERS Int. Solid-State Sensors, Actuators Microsyst. Conf.*, 2007, pp. 1385–1388. doi: 10.1109/SENSOR.2007.4300401.
[10] S. Choi et al., "Thin-film transistor-driven vertically stacked full-color organic light-emitting diodes for high-resolution active-matrix displays," *Nat. Commun.*, vol. 11, no. 1, Jun. 2020, Art. no. 2732, doi: 10.1038/s41467-020-16551-8.
[11] T. P. Brody, "The thin film transistor—A late flowering bloom," *IEEE Trans. Electron Devices*, vol. 31, no. 11, pp. 1614–1628, Nov. 1984, doi: 10.1109/T-ED.1984.21762.
[12] L. Hofmann, M. Ebert, P. A. Tass, and C. Hauptmann, "Modified pulse shapes for effective neural stimulation," *Front. Neuroeng.*, vol. 4, Sep. 2011, doi: 10.3389/fneng.2011.00009.
[13] T. J. Foutz and C. C. McIntyre, "Evaluation of novel stimulus waveforms for deep brain stimulation," *J. Neural Eng.*, vol. 7, no. 6, Dec. 2010, Art. no. 066008, doi: 10.1088/1741-2560/7/6/066008.
[14] M. A. Hays et al., "Towards optimizing single pulse electrical stimulation: High current intensity, short pulse width stimulation most effectively elicits evoked potentials," *Brain Stimul.*, vol. 16, no. 3, pp. 772–782, May/Jun. 2023, doi: 10.1016/j.brs.2023.04.023.
[15] M. Berggren and G. G. Malliaras, "How conducting polymer electrodes operate," *Science*, vol. 364, no. 6437, pp. 233–234, Apr. 2019, doi: 10.1126/science.aaw9295.
[16] H. A. Yigit, H. Ulusan, S. Chamanian, and H. Kulah, "Charge balance circuit for constant current neural stimulation with less than 8 nC residual charge," in *Proc. IEEE Int. Symp. Circuits Syst. (ISCAS)*, 2019, pp. 1–5. doi: 10.1109/ISCAS.2019.8702790.
[17] W. Wang et al., "Neuromorphic sensorimotor loop embodied by monolithically integrated, low-voltage, soft e-skin," *Science*, vol. 380, no. 6646, pp. 735–742, May 2023, doi: 10.1126/science.ade0086.
[18] V. Benfenati et al., "A transparent organic transistor structure for bidirectional stimulation and recording of primary neurons," *Nat. Mater.*, vol. 12, no. 7, pp. 672–680, Jul. 2013, doi: 10.1038/nmat3630.
[19] I. Uguz and K. L. Shepard, "Spatially controlled, bipolar, cortical stimulation with high-capacitance, mechanically flexible subdural surface microelectrode arrays," *Sci. Adv.*, vol. 8, no. 42, Oct. 2022, Art. no. eabq6354, doi: 10.1126/sciadv.abq6354.
[20] D. Satzer, D. Lanctin, L. E. Eberly, and A. Abosch, "Variation in deep brain stimulation electrode impedance over years following electrode implantation," *Stereotact. Funct. Neurosurg.*, vol. 92, no. 2, pp. 94–102, 2014, doi: 10.1159/000358014.